OUKA
The University of Osaka
Institutional Knowledge Archive

Title	Effects of autogenous bone graft on mass and quality of trabecular bone in Ti-6Al-4V spinal cage fabricated with electron beam melting
Author(s)	Takahashi, Hiroyuki; Ishimoto, Takuya; Inoue, Takayuki et al.
Citation	Materials Transactions. 2019, 60(1), p. 144-148
Version Type	VoR
URL	https://hdl.handle.net/11094/89901
rights	
Note	

The University of Osaka Institutional Knowledge Archive : OUKA

https://ir.library.osaka-u.ac.jp/

The University of Osaka

Materials Transactions, Vol. 60, No. 1 (2019) pp. 144 to 148
©2018 The Japan Institute of Metals and Materials

Effects of Autogenous Bone Graft on Mass and Quality of Trabecular Bone in Ti–6Al–4V Spinal Cage Fabricated with Electron Beam Melting

Hiroyuki Takahashi[1,*1], Takuya Ishimoto[2], Takayuki Inoue[1], Hiroomi Kimura[1], Keita Uetsuki[1], Natsuki Okuda[2,*1], Yohei Nakanishi[2,*1], Jong Yeong Oh[2,*1], Manabu Ito[3], Yoshio Nakashima[1], Takao Hanawa[4] and Takayoshi Nakano[2,*2]

[1]*Teijin Nakashima Medical Co. Ltd., Okayama 709-0625, Japan*
[2]*Division of Materials and Manufacturing Science, Graduate School of Engineering, Osaka University, Suita 565-0871, Japan*
[3]*Hokkaido Medical Center, Sapporo 063-0005, Japan*
[4]*Department of Metallic Biomaterials, Institute of Biomaterials and Bioengineering, Tokyo Medical and Dental University, Tokyo 101-0062, Japan*

A spinal cage is one of the primary spinal devices used for the treatment of spinal diseases such as lumbar spondylolisthesis. Since it is set in the intervertebral space that causes instability to promote the fusion of the adjacent vertebral bodies, it requires the early induction of healthy bones. For this reason, in most cases, an autogenous bone extracted from the patient's ilium is implanted in the interior of the cage to stimulate bone formation. However, collecting autogenous bone involves secondary surgery and several clinical problems such as pain in the part from which it is collected. Additionally, the effect of the autogenous bone graft itself has not been sufficiently studied yet. Moreover, the mechanical functions of trabecular bones in a vertebral body are governed by the anisotropic structure of the trabeculae and the preferential orientation of the apatite/collagen in a trabecula with respect to the principal stress. Despite this fact, after the implantation of the cage, the mass of the bones is evaluated with soft X-ray photography, which does not guarantee an accurate measurement of bone functions. In this study, the effect of the autogenous bone graft on the spinal cage was verified based on structural anisotropy of trabecular bones and the preferential orientation of apatite/collagen in a trabecula using sheep. The autogenous bone graft demonstrated a significant effect on the increase of bone mass and anisotropy of the trabecular structure. However, compared to the trabecular anisotropy of normal parts, the anisotropy of the trabecular structure and apatite *c*-axis orientation of the parts with autogenous bone graft were considerably lower, indicating a minimal effect of the autogenous bone graft. Therefore, it was suggested that early stabilization of the spinal cage requires another strategy that rapidly forms the unique hierarchical anisotropic structure of trabecular bones. [doi:10.2320/matertrans.M2018329]

(Received October 15, 2018; Accepted October 25, 2018; Published November 23, 2018)

Keywords: *intervertebral cage, trabecular bone, bone quality, collagen/apatite orientation, trabecular anisotropy*

1. Introduction

A spinal cage is one of the primary spinal implant devices used for the treatment of diseases such as degenerative spondylolisthesis, which cause neuropathy due to a destabilized vertebral body. Because it is inserted in an intervertebral space to fuse and stabilize the adjacent vertebral bodies, it is also referred to as an intervertebral fusion cage. The number of patients who used a spinal cage in Japan was more than 70,000 in 2017, and this figure is expected to increase in the future as the population ages.[1)]

Since a spinal cage stabilizes the vertebral bodies, it is essential that there is a rigid fusion between the cage and vertebral bone. The most common shape of a spinal cage currently used is the box type, which has a large cavity in the central part to accelerate fusion with the adjacent vertebrae. In most cases, this cavity is filled with grafted bone extracted from the ilium to stimulate osteointegration.[2)] However, extracting a bone graft from the ilium is an invasive and burdensome procedure for the patient, and the pain occurs at the harvest site of iliac crest bone graft after the surgery, which are clinical problems associated with autogenous bone graft.[3,4)] For this reason, it is necessary to develop a new spinal cage that stimulates osteointegration and provides strong mechanical fixation without the use of autogenous bones. In practice, however, the effects of autogenous bone graft on mechanical fixation have not been sufficiently studied yet.[5)]

The mechanical functions of a bone are governed not only by its mass but also by bone quality partly characterized by the preferential orientation of bone matrix, which mainly consists of collagen and apatite.[6–8)] Since a vertebral body contains abundant trabecular bones, the mechanical fixation between the cage and bones is determined by the structural anisotropy of the trabeculae and the preferential orientation of collagen/apatite within it. Therefore, these indices can be used as new indices to evaluate the soundness of trabecular bones.[9)] Through the construction of anisotropic trabeculae that runs along the trajectory of principal stress, as well as the anisotropic material of the trabecula,[10)] the mechanical properties of trabecular bones in the stress direction were improved. However, the evaluation of the bone after the implantation of the spinal cage is performed based on the bone mass by soft X-ray photography, X-ray computed tomography (CT), and histopathological tissue examination.

In this study, we performed a cage implantation test in a sheep with a standard box-type spinal cage to clarify the effects of autogenous bone graft using new evaluation indices: trabecular structure anisotropy and preferential orientation of collagen/apatite within the trabecula.

2. Materials and Methods

2.1 Design and construction of a spinal cage for a sheep

In this study, to construct a spinal cage with the shape and

*[1]Graduate Student, Osaka University
*[2]Corresponding author, E-mail: nakano@mat.eng.osaka-u.ac.jp

size of the vertebral body of the sheep used, we designed it using previously acquired micro-CT images of sheep spine. The cage was designed with a width of 12 mm and a length of 23 mm to prevent deviation of the cage from the anterior edge of the vertebral body and interference between cage and spinal canal (spinal nerve). The height of the cage was set to 7 mm. This is adequately higher than the soft tissues including the intervertebral disk. Two cavities, which were each 6 mm wide and 6.5 mm long, were created in the interior of the cage. Additionally, to increase the fluidity of the bone marrow, a through hole with a diameter of 1.5 mm was created on the side of these cavities (Fig. 1). The cage was constructed with Ti–6Al–4V ELI (extra low interstitial) alloy powder based on computer-aided design (CAD) (SolidWorks; Dassault Systèmes SolidWorks, France) data. The cage was fabricated with the electron beam melting (EBM) method (Model Q10; Arcam, Sweden),[11] one of the layer-by-layer powder bed fusion type metal 3D-printers in which a thin layer of metal powder is selectively melted by an electron beam irradiation to form 3D structures.

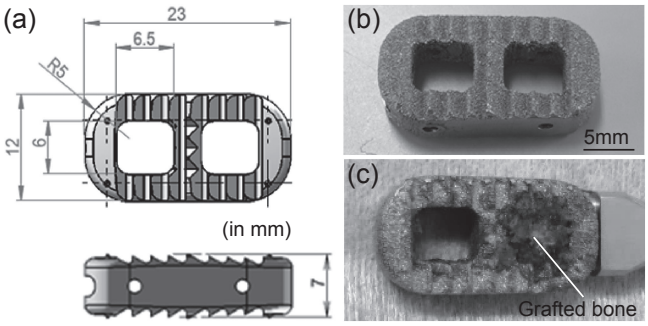

Fig. 1 (a) Schematics representing shape and dimensions of the spinal cage and (b) picture of fabricated cage by electron beam melting. (c) Autogenous iliac bone graft on one side of the cavities.

2.2 Implantation of the spinal cage in the sheep spine

Five 18-months-old male Suffolk sheep weighting 72 ± 6 kg were used in the experiment. They were fixed in the lateral decubitus position under inhalation anesthesia. The spinal cage was implanted in the space between lumbar vertebral body L1–L2 and L3–L4 (Fig. 2) through a lateral approach. With a box chisel, the intervertebral disks were partially cut according to the shape of the cage which was implanted in that cut part. Pedicle screws were attached to the vertebral body adjacent to the affected part, and the implanted spinal cage was compressed by connecting these screws with a rod. To analyze the effects of autogenous bone graft under similar conditions, one of the cavities in the spinal cage was filled with autogenous bone extracted from the ilium (bone graft (BG) group), and the other was left empty (control group) (Fig. 1(c)). After removing the fibrous soft tissue, the autogenous bone was crushed into pieces with a size of 2–3 mm using a bone rongeur. The autogenous bone was filled in the cage cavity without any additional treatments.

The implantation period was set to eight weeks so that the initial osteointegration behavior could be analyzed. In the eighth week after the surgery, calcein green (25 mg/kg) was administered intravenously, and the bones were fluorescent-labeled. Eight weeks after the implantation, the animals were euthanized (pentobarbital, 20 mg/kg, intravenous administration), and the cages were removed along with the surrounding bones. The bones were immersed in 70% ethanol and fixated. All experimental procedures were approved by the Institutional Review Board of the Bioscience Department/Toya Laboratory of Hokudo Co., Ltd.

2.3 Analysis of bones around and inside the spinal cage

Based on the analysis of the bones around and inside the spinal cage, two types of undecalcified thin slices in the sagittal section were obtained to evaluate the effect of the autogenous bone transplantation. The first type was a histopathological tissue slice, which was stained with Villanueva bone stain, embedded in methyl methacrylate resin, and polished to a thickness of 100 μm. It was placed under visible and fluorescent light to observe bone formation activity and bone morphology. The second type was a 1-mm-thick slice obtained from the part adjacent the histopathological slice. The trabecula was photographed using the micro-CT method (SMX-100CT, Shimadzu, Japan), and the amount of trabecular bone determined as percent of bone volume with respect to total bone volume (BV/TV) and degree of anisotropy of the trabecular structure along the craniocaudal axis were quantitatively analyzed using the 3D analysis software TRI-3D BON (Ratoc System Engineering, Japan). The degree of trabecular anisotropy was quantitatively determined from the aspect ratio of fabric ellipsoid (major axis length/minor axis length) calculated from the mean intercept length.[9] Additionally, the apatite *c*-axis orientation in the trabecula within the X-ray irradiation area was analyzed with a microbeam X-ray diffractometer (R-Axis BQ; Rigaku, Japan) that has a transmission optical system. The Mo-Kα was used as a radiation source. The collimator diameter was 800 μm and the measurement time was 300 seconds. The incident beam was irradiated vertically to sliced sample to obtain the two-dimensional diffraction intensity distribution (Debye ring) on the slice surface.[12] The integrated diffraction intensity (I) from the crystal plane (002) representing the *c*-axis and that from (310) perpendicular to (002) were obtained at every azimuth angle (β) of 1°. The β dependency of each diffraction intensity was approximated by the least square method with the modified ellipsoid function below

$$I(\beta) = \left\{ \frac{\cos^2(\beta - \mu)}{a^2} - \frac{\sin^2(\beta - \mu)}{b^2} \right\}^{-\frac{1}{2}} - c \qquad (1)$$

and the integrated diffraction intensity ratio I (002)/I (310) was calculated for each β.[13] a, b, c, and μ are constants. This enables to analyze the direction and magnitude of maximum apatite *c*-axis orientation within the plane. Moreover, the preferential orientation of apatite *c*-axis reflects that of collagen fibers because apatite crystallizes on the collagen template in an epitaxial manner through an *in vivo* self-assembly process so that apatite *c*-axis is parallel to the elongated direction of collagen.[14]

The numerical data obtained from each analysis above is represented as the mean value ± standard error. The mean values were considered statistically significant when $P < 0.05$. Data were analyzed using repeated measures analysis

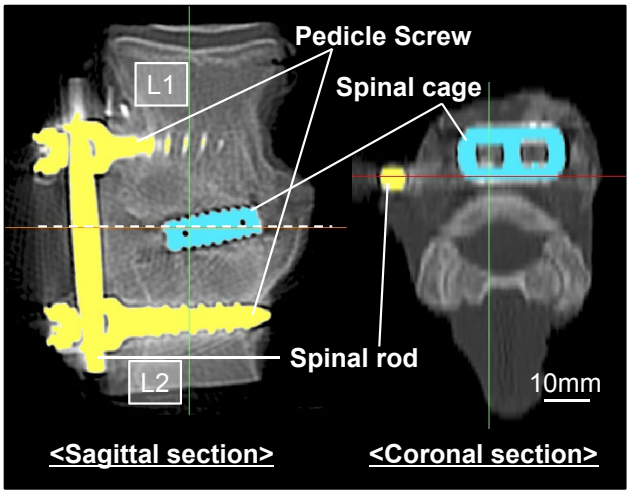

Fig. 2 Computed tomography images of spinal cage after implantation into the intervertebral space.

of variance (IBM SPSS software for Microsoft Windows version 25 (SPSS Japan Inc., Japan)).

3. Results and Discussion

All the animals started walking less than one hour after the surgery, and no infection was observed during the test period. In this study, we designed and produced an intervertebral spinal cage with two cavities and verified whether the autogenous bone graft had any effect on bone fusion through the cavities.

Micro-CT was used to confirm that the spinal cage was implanted in the intervertebral space of the extracted spine (Fig. 2). Figure 3 shows images of the sagittal section, including the cage, stained with Villanueva bone stain and green-fluorescent calcein. No soft tissue was observed between the cage and the adjacent vertebral body, indicating that the height of the cage was appropriate. Bone ingrowth from the adjacent vertebral body was observed in the cage cavity, regardless of the autogenous bone. Since calcein combines with calcium, fluorescent coloring were observed in bone that calcified when the calcein was administered. From the image of the calcein staining (Fig. 3(b)), we noted that, the bone formation activity after the cage implantation was limited to the interior and a small peripheral part of the cage.

Figure 4 shows micro-CT images of bone tissue from inner regions of the cavities in the cage and bone tissue 7 mm distant from the cage surface. Since almost no calcein coloring was detected in the distant region, we referred to this distant region as the normal part, which was hardly influenced by the implantation of the cage.[9] The morphology of the trabeculae in the inner and distant regions was very different. While the trabeculae preferentially run along the craniocaudal axis in the distant region, the trabecular structure was less anisotropic and the trabecula was thin in the inner regions, regardless of the transplanted autogenous bone.

The BV/TV and degree of trabecular anisotropy of the inner and distant regions are shown in Fig. 5. The data from the distant region is indicated by the broken line. The BV/TV of the BG group was significantly higher than that of the control group. Additionally, even though the trabecular

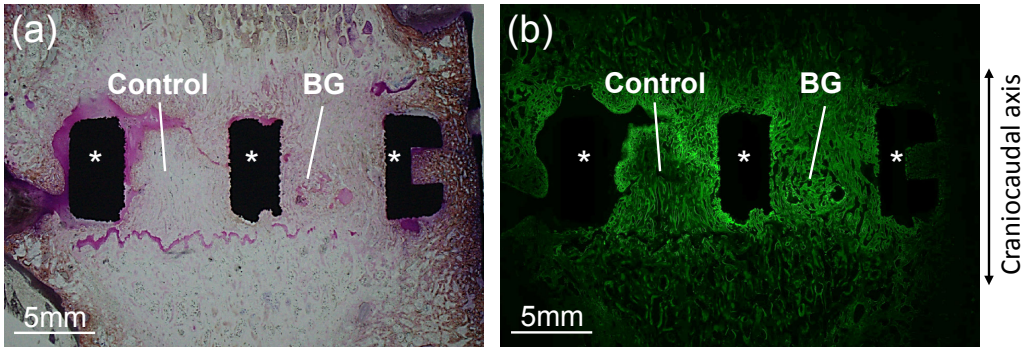

Fig. 3 (a) Villanueva bone stain image and (b) calcein fluorescent image of sagittal section including spinal cage cavities. *: cross-section of Ti–6Al–4V cage.

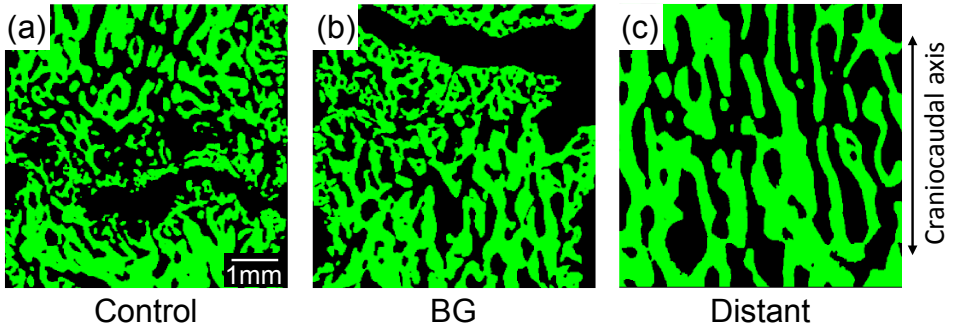

Fig. 4 Micro-X-ray computed tomography cross-sectional images of vertebral trabecular bone from (a) inner regions of the cage of control group and (b) BG group, and (c) distant region.

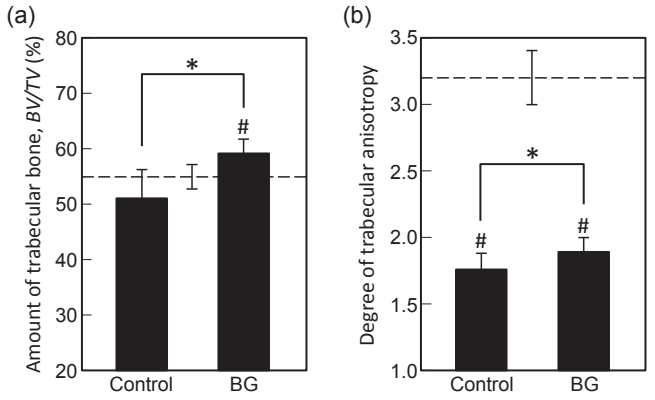

Fig. 5 (a) Amount of trabecular bone (BV/TV) and (b) degree of trabecular anisotropy from inner regions of the cage in control and BG groups (bars) and distant region (broken line). *: $P < 0.05$. #: $P < 0.05$ vs distant region.

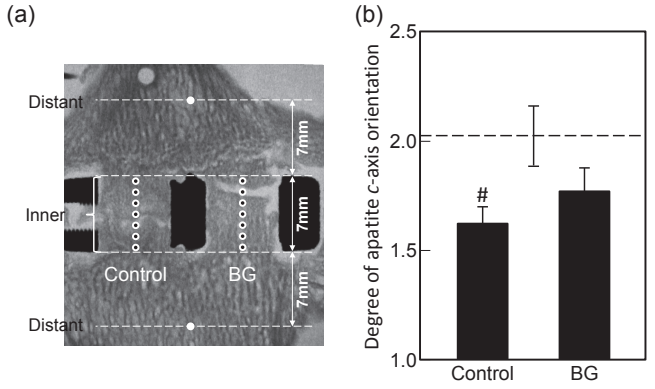

Fig. 6 (a) Representation of analyzed points and (b) degree of apatite *c*-axis orientation analyzed in the inner regions of the cage in control and BG groups (bars) and distant region (broken line). #: $P < 0.05$ vs distant region.

anisotropy was significantly high in the BG group, it was considerably lower than that of the distant region in both groups.

Figure 6 shows the apatite crystallographic *c*-axis orientation along the craniocaudal axis. For each animal, the mean value from seven points in the inner region and from two points in the distant region was used. Even though there was no significant difference between the control group and the BG group, the control group without autogenous bone graft showed a significantly low orientation in the distant region.

The aforementioned results indicate that autogenous bone graft can effectively increase the amount of bone formation and trabecular structure anisotropy in the craniocaudal axis. The fact that the trabecular bones form the preferential trabecular directionality along the principal stress direction through remodeling suggests that the cellular components and various cytokines contained in grafted bones, including bone marrow, contributed to the increase in the remodeling activity. However, the anisotropy and apatite orientation of the trabecular structure in the inner part was very low. We, therefore, conclude that the effect of the autogenous bone graft on the initial recovery in mechanical function is minor in this case.

A strategy for the reconstruction of the unique hierarchical anisotropy of the trabecular bone should be required for early stabilization of the spinal cage. Other studies have reported the use of growth factors such as bone morphogenetic protein-2 to accelerate the fusion, and soft X-ray photographs indicated a high fusion rate.[15,16] However, since these photographs only allow for a quantitative evaluation of bone mass, it is unclear whether the bone is mechanically sound. The use of growth factors increases bone formation activity dramatically. On the other hand, it has been reported that growth factors lead to the formation of bones with low orientation and inferior mechanical functions.[8,17] A different strategy other than use of growth factors is required for the early recovery of bone anisotropy.

For example, the elongation and alignment of the osteoblasts, which form bones, is extremely important for the matrix orientation in bones. Bone matrix is formed in parallel with the aligned direction of the osteoblasts and the higher osteoblast alignment results in the more prominent bone matrix orientation.[18] It is also possible to obtain aligned osteoblasts from undifferentiated cells such as induced pluripotent stem (iPS) cells.[19] The arrangement of osteoblasts can be controlled with fine anisotropic grooves on the substrate.[20,21] The challenge is how to introduce a surface with such a fine structure into the interior of the spinal cage. Moreover, implant devices that is suited to respective spinal bone defects created, for example, by resection of cancer metastasis[22–26] will gain more importance in the future. 3D printers which enable to fabricate 3D structure with high flexibility in product shape and high precision should be one of the solutions.

The validity of the sheep model for the study of the spinal devices for human should be discussed. As humans are bipeds and sheep are quadrupeds, the craniocaudal axis directions of their spines are vertical and horizontal, respectively, to the ground. However, the anatomical shape of the sheep spine is similar to that of humans,[27] and both have a trabecula that runs in parallel with the craniocaudal axis. This also supports the assumption that the direction of principal stress in the vertebral bodies of humans and sheep is similar with respect to the craniocaudal axis.[28] In the case of quadrupedal animals, bending moment is applied on the spine, which is converted to an axial load on the craniocaudal axis. Based on these facts, we can say that studies involving sheep are useful for the research and development of spinal devices for humans.

4. Conclusion

In this study, we used sheep to verify the effect of transplanting autogenous bone into cavities in a spinal cage with a hollow structure. The results indicated that transplanted autogenous bone could increase the bone mass and anisotropy of the trabecular structure. However, compared to a normal part, the trabecular structure anisotropy and apatite orientation were considerably low, even after autogenous bone transplantation. Therefore, the results suggest that a strategy for the reconstruction of the unique layered anisotropy of the trabecular bone for early stabilization of the spinal cage is required.

Acknowledgement

The authors (H. Takahashi and T. Ishimoto) contributed equally to this work. This study was supported by Strategic Promotion of Innovative Research and Development (S-Innovation) from the Japan Agency for Medical Research and Development (AMED), and the Grants-in-Aid for Scientific Research S (JP18H05254) from the Japan Society for the Promotion of Science (JSPS), and the Light Metal Educational Foundation.

REFERENCES

1) Yano Research Institute: Medical Bionics (Artificial Organs) Market 2017 (2018).
2) A.M.T. Chau and R.J. Mobbs: Eur. Spine J. **18** (2009) 449–464.
3) D.H. Kim, R. Rhim, L. Li, J. Martha, B.H. Swaim, R.J. Banco, L.G. Jenis and S.G. Tromanhauser: Spine J. **9** (2009) 886–892.
4) C.E. Schwartz, J.F. Martha, P. Kowalski, D.A. Wang, R. Bode, L. Li and D.H. Kim: Health Qual. Life Outcomes **7** (2009) 49.
5) A.M.T. Chau, L.L. Xu, J.H.-Y. Wong and R.J. Mobbs: Neurosurg. Rev. **37** (2014) 23–37.
6) T. Nakano, K. Kaibara, Y. Tabata, N. Nagata, S. Enomoto, E. Marukawa and Y. Umakoshi: Bone **31** (2002) 479–487.
7) T. Nakano, K. Kaibara, T. Ishimoto, Y. Tabata and Y. Umakoshi: Bone **51** (2012) 741–747.
8) T. Ishimoto, T. Nakano, Y. Umakoshi, M. Yamamoto and Y. Tabata: J. Bone Miner. Res. **28** (2013) 1170–1179.
9) T. Ishimoto, K. Yamada, H. Takahashi, M. Takahata, M. Ito, T. Hanawa and T. Nakano: Bone **108** (2018) 25–33.
10) S. Miyabe, T. Nakano, T. Ishimoto, N. Takano, T. Adachi, H. Iwaki, A. Kobayashi, K. Takaoka and Y. Umakoshi: Mater. Trans. **48** (2007) 343–347.
11) T. Nakano and T. Ishimoto: KONA Powder Particle J. **32** (2015) 75–84.
12) T. Ishimoto, B. Sato, J.-W. Lee and T. Nakano: Bone **103** (2017) 216–223.
13) Y. Noyama, T. Nakano, T. Ishimoto, T. Sakai and H. Yoshikawa: Bone **52** (2013) 659–667.
14) W.J. Landis: Bone **16** (1995) 533–544.
15) B. McKay and H.S. Sandhu: Spine **27** (2002) S66–S85.
16) M. Lykissas and I. Gkiatas: World J. Orthop. **8** (2017) 531–535.
17) M. Kashii, J. Hashimoto, T. Nakano, Y. Umakoshi and H. Yoshikawa: J. Bone Miner. Metab. **26** (2008) 24–33.
18) A. Matsugaki, Y. Isobe, T. Saku and T. Nakano: J. Biomed. Mater. Res. A **103** (2015) 489–499.
19) R. Ozasa, A. Matsugaki, Y. Isobe, T. Saku, H.-S. Yun and T. Nakano: J. Biomed. Mater. Res. A **106** (2018) 360–369.
20) A. Matsugaki, G. Aramoto, T. Ninomiya, H. Sawada, S. Hata and T. Nakano: Biomaterials **37** (2015) 134–143.
21) A. Matsugaki, G. Aramoto and T. Nakano: Biomaterials **33** (2012) 7327–7335.
22) A. Sekita, A. Matsugaki and T. Nakano: Mater. Trans. **57** (2016) 2077–2082.
23) Y. Kimura, A. Matsugaki, A. Sekita and T. Nakano: Sci. Rep. **7** (2017) srep44824.
24) A. Sekita, A. Matsugaki, T. Ishimoto and T. Nakano: J. Struct. Biol. **197** (2017) 260–270.
25) R. Wei, W. Guo, T. Ji, Y. Zhang and H. Liang: Eur. Spine J. **26** (2017) 1902–1909.
26) A. Sekita, A. Matsugaki and T. Nakano: Bone **97** (2017) 83–93.
27) H.J. Wilke, A. Kettler, K.H. Wenger and L.E. Claes: Anat. Rec. **247** (1997) 542–555.
28) Y. Wang, G. Liu, T. Li, Y. Xiao, Q. Han, R. Xu and Y. Li: Comp. Med. **60** (2010) 374–379.